Fracture Mechanics of Concrete Structures, de Borst et al (eds) © 2001 Swets & Zeitlinger, Lisse, ISBN 90 2651 825 0

Time-Dependent Fracture of Concrete using Fractional Order Rate Laws

Fabrizio Barpi & Silvio Valente
Department of Structural and Geotechnical Engineering, Politecnico di Torino, Torino, Italy

ABSTRACT: The interaction between strain-softening and time-dependent behaviour is analysed in the case of quasi-static fracture. A fractional order rate law is coupled with a micromecanical model for the fracture process zone. In this way, a whole range of dissipative mechanisms is included in a single viscous element. This problem is analised through the finite element method and the cohesive (or fictitious) crack model. The comparison with creep tests executed on prenotched beams shows a good agreement.

1 INTRODUCTION

The long term performance of concrete structures is fundamentally affected by the behaviour of the material after cracking. In the concrete, instead of a well defined crack tip, there is a diffused damage zone within which micro-cracking increases and stresses decrease as the overall deformation increases. This results in the softening of the material in the so called *fracture process zone* (FPZ). The size of this zone can be compared with a characteristic dimension of the structure and can vary during the evolutionary process. In this context, a numerical method (based on finite or boundary elements) has to be used together with the cohesive or fictitious crack model (Barenblatt (1959), Dugdale (1960) and Hillerborg et al. (1976)).

The interaction between strain-softening and time dependent behaviour is analysed, with the emphasis on very slow or quasi-static fracture. This is the case of cracking in massive concrete structures like dams, where inertial forces can be neglected.

For this problem, three approaches have been proposed. The first is based on the concept of *activation energy* and *rate dependent softening* and has been developed in a series of papers by Bažant and coworkers (Bažant and Jiràsek (1993), Bažant and Gettu (1992), Wu and Bažant (1993)).

The second approach is based on the inclusion of a *rheological model* for creep and relaxation, whose mechanical properties are obtained by fitting experimental tests (Hansen (1991), Zhou and Hillerborg (1992), Carpinteri et al. (1995), Barpi et al. (1998)).

The third is based on a *micromechanical* model which combines time-dependent and time-independent information. One of these models was proposed by Santhikumar and Karihaloo (1996), Santhikumar et al. (1998). The time-independent part of this model is based on the concept of *effective spring*, which derives from a micromechanical model for the static softening behaviour of the concrete in the fictitious process zone proposed by Huang and Li (1989). In the present paper this approach is enhanced using a *fractional order* rate law and is applied to the numerical simulation of the three-point bending tests described by Zhou (1992).

2 RHEOLOGICAL MODEL

Rheology is concerned with time dependent deformation of solids. The first problem that arises is how complex the linear viscoelastic model must be, i.e., what is the minimum number of material parameters that is required for an accurate description of the observed material behaviour. It has been argued, see Bagley and Torvik (1983), that it is sufficient to use as few as four parameters for the uniaxial stress situation (two elastic constants, one relaxation constant and the non-dimensional fractional order of differentiation).

Figure 1 represents the simplest rheological model of the linear standard viscoelastic solid.

The springs are characterized by linear stress-displacement relationships defined by Hooke's law with constant moduli of elasticity E_1 and E_2:

$$\sigma_1 = E_1(w - q_1), \tag{1a}$$

$$\sigma_2 = E_2\, w. \tag{1b}$$

The dashpot is based on fractional derivative operator of order $\alpha \in (0,1)$:

$$D^\alpha q_1 = \frac{\sigma_1}{E_1\, \tau_1^\alpha} = \frac{w - q_1}{\tau_1^\alpha}, \tag{2}$$

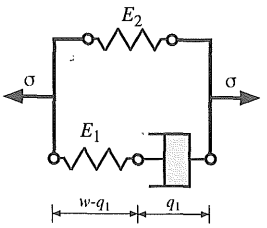

Figure 1: Linear standard viscoelastic solid.

where the fractional differentiation of a function $y(t)$ is defined according to Gel'fand and Shilov (1964) and Oldham and Spanier (1974) (see also Carpinteri and Mainardi (1997)).

In particular:

$$D^{-(1-\alpha)}y(t) = \int_0^t \Phi_{1-\alpha}(t-\bar{t})\, y(\bar{t})\mathrm{d}\bar{t}, \qquad (3)$$

where:

$$\Phi_{1-\alpha}(t) = \frac{t_+^{-\alpha}}{\Gamma(1-\alpha)} \quad \text{with} \quad t_+ = \begin{cases} t & \text{if} \quad t > 0 \\ 0 & \text{if} \quad t < 0 \end{cases} \qquad (4)$$

In the previous expression Γ represents the *Gamma function*. A convergent expression for the α-order fractional derivative operator D^α is given by:

$$\begin{aligned} D^\alpha y(t) &= D^1 D^{-(1-\alpha)} y(t) = \\ &= \frac{\mathrm{d}}{\mathrm{d}t}\int_0^t \Phi_{1-\alpha}(t-\bar{t})\, y(\bar{t})\mathrm{d}\bar{t} = \\ &= \frac{1}{\Gamma(1-\alpha)}\frac{\mathrm{d}}{\mathrm{d}t}\int_0^t \frac{y(\bar{t})}{(t-\bar{t})^{-\alpha}}\mathrm{d}\bar{t}, \end{aligned} \qquad (5)$$

In the case of $\alpha = 1$ the classical dashpot with an integer order rate law is obtained from Eq. 2. In particular the solutions for the relaxation problem (under constant w) and for the creep problem (under constant σ) become of exponential type, with τ_1 as the *relaxation time*, and $\tau_1 \frac{E_1+E_2}{E_2}$ as the *retardation time*.

The normalized stress relaxation functions $\frac{\sigma(rel)}{\sigma(t=0)}$ vs. non-dimensional time $\frac{t}{\tau_1}$ are plotted in Fig. 2 for the case $E_1 = E_2$ while the normalized creep functions $\frac{w(creep)}{w(t=0)}$ vs. non-dimensional time $\frac{t}{\tau_1}$ are plotted in Fig. 3 for the case $E_1 = E_2$.

2.1 *Numerical integration of constitutive response*

A possible approximation for the fractional differentiation of a function $y(t)$ is (see Oldham and Spanier (1974)) :

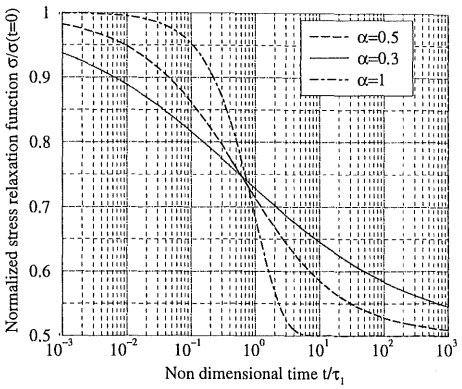

Figure 2: Stress relaxation function.

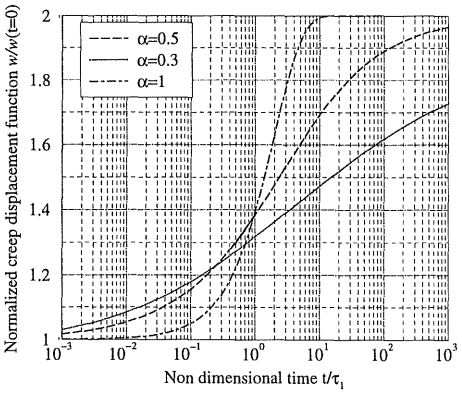

Figure 3: Creep displacement function.

$$^{n+1}(D^\alpha y) = \frac{1}{(\Delta t)^\alpha}\sum_{j=0}^{n} b_j(\alpha)\, ^{n+1-j}y, \qquad (6)$$

with:

$$^n y = y(n\Delta t), \qquad (7)$$

and

$$b_j(\alpha) = \frac{\Gamma(j-\alpha)}{\Gamma(-\alpha)\Gamma(j+1)}. \qquad (8)$$

The following recursion formula simplifies the calculation of $b_j(\alpha)$:

$$\frac{\Gamma(j-\alpha)}{\Gamma(j+1)} = \frac{(j-1-\alpha)}{j}\frac{\Gamma(j-1-\alpha)}{\Gamma(j)}. \qquad (9)$$

The coefficients $b_j(\alpha)$ are given by:

$$b_0(\alpha) = 1, \quad b_1(\alpha) = -\alpha, \ldots,$$

$$b_k(\alpha) = \frac{(k-1-\alpha)}{k} b_{k-1}(\alpha), \ldots \qquad (10)$$

This finite difference approximation is applied to Eq. 2, and integrated over time, using the *General Midpoint Rule* (see Enelund et al. (1999)).

3 FICTITIOUS PROCESS ZONE

In each point of the fictitious process zone a micromechanical approach to tension softening is combined with the above rheological model according to a strategy proposed by Santhikumar and Karihaloo (1996) and Santhikumar et al. (1998).

3.1 *Micromechanical model*

Tension softening behaviour appears when the damage in the material has localized along eventual fracture planes. This behaviour has been successfully modelled using two- and three-dimensional micromechanical models (Huang and Li (1989), Karihaloo (1995)). All models provide a relationship between the residual tensile stress carrying capacity and crack opening displacement (COD) as a function of known concrete microstructural parameters, e.g. aggregate volume fraction V_f, Young's modulus E_c, ultimate tensile strength f_t and fracture toughness of the homogenized material K_{Ic}^{hom} (see Fig. 4). According to these models, the function is assumed to be:

$$\frac{w}{w_c} = \underbrace{\frac{(K_{Ic}^{hom})^2}{E_c(1-V_f)f_t}}_{\beta} \frac{f_t}{\sigma} \left[1 - \left(\frac{\sigma}{f_t}\right)^3\right]. \qquad (11)$$

All the microstructural material parameters are included in the factor β.

During the loading phase each point of the FPZ moves on the same stress-COD curve. Later on this condition does not hold any longer, due to the combined effect of *viscosity* and *damage*. Analogously, during the loading phase all pairs (σ, w) are located on the above mentioned curve and during the load sustained phase this condition does not hold any longer.

4 INTERACTION BETWEEN RHEOLOGICAL AND MICROMECHANICAL MODELS

In order to understand how the rheological and micromehanical models interact, three simple cases are analized:

1. if the displacement discontinuity w is kept constant along time step Δt, a stress relaxation $\Delta\sigma$ occurs according to the standard viscoelastic element described;

2. if the stress σ is kept constant along time step Δt, a creep displacement Δw occurs according to the standard viscoelastic element described;

3. if both stress σ and displacement discontinuity w are forced to stay on the static curve (Eq. 6 and Fig. 4) one of the two increments occurs as predicted by the rheological element, while the other is equal or smaller.

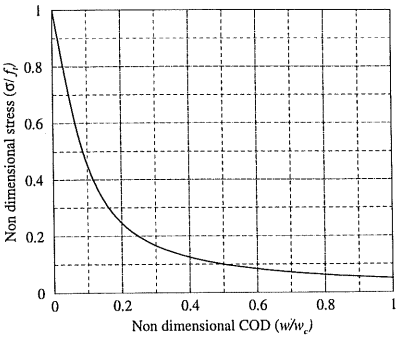

Figure 4: Cohesive stress-COD law ($\beta = 0.05$).

Figure 5 shows the stiffnesses for the two basic cases. In greater detail, for the first case the unloading stiffness is assumed (effective spring hypothesis) while, for the second case, the stiffness tangent to the stress-COD curve $\frac{|d\sigma|}{dw}$ is taken into account.

At the end of each time step, the microcrack pattern changes and both stiffnesses are updated, as shown in Fig. 5 (where both of them are reduced). It is worth noting that each point follows a different path and, hence, exibits a different stiffness, while $E_1 = E_2$ and $\tau_1$is constant. A creep increment of β induces the dotted curve in Fig. 5 (right).

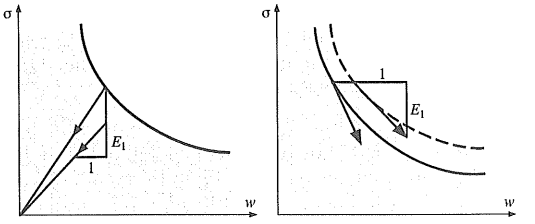

Figure 5: Stress paths and associated stiffnesses.

The previous three cases concern a single degree of freedom system. The related response diagrams, for integer order rate laws ($\alpha = 1$) were published by Santhikumar and Karihaloo (1996) and Santhikumar et al. (1998).

5 GLOBAL ANALYSIS

In the present work, the continuum surrounding the process zone is assumed as *linear elastic*. All non-linear and time-dependent phenomena are assumed to occur in the process zone. When the fictitious crack tip advances by a pre-defined length, each point located on the crack trajectory, is split into two points. The virtual mechanical entity, acting on these two points only, is called *cohesive element*. The local behaviour of such an element follows the rules mentioned in the previous section. Each cohesive element interacts with the others only through the undamaged continuum, external to the process zone. According to the finite element method, by taking the unknowns to be the n nodal displacement increments, $\Delta \boldsymbol{u}$, and assuming that compatibility and equilibrium conditions are satisfied at all points in the solid, we get the following system of n equations with $n+1$ unknowns ($\Delta \boldsymbol{u}$, $\Delta\lambda$ or Δt).

The creep effect is incorporated by simply adding the pseudo-load induced by relaxation to the load vector in the equilibrium equations (Bocca et al. (1991), Barpi et al. (1999)):

$$(\boldsymbol{K}_T + \boldsymbol{C}_T)\,\Delta \boldsymbol{u} = \Delta\lambda\,\boldsymbol{P} + \Delta t\,\boldsymbol{Q}, \qquad (12)$$

where:

- $\boldsymbol{K}_T$: positive definite tangential stiffness matrix, containing contributions from linear elastic (undamaged) elements and possible contributions from cohesive elements having (σ, w) below the curve of Fig 4. The conditions in which this possibility applies will be described later on;
- $\boldsymbol{C}_T$: negative definite tangential stiffness matrix, containing contributions from cohesive elements with (σ, w) on the curve of Fig 4;
- $\boldsymbol{P}$: the vector of external load;
- $\Delta\lambda$: maximum load multiplier which is compatible with Eq. 11 and the fictitious crack tip growth condition ($\sigma = f_t$);
- $\boldsymbol{Q}$: vector of unbalanced load (or pseudo-load) due to relaxation in the process zone, related to a unitary time increment.

During the loading phase, the behaviour of the material is assumed to be time-independent ($\boldsymbol{Q} = \boldsymbol{0}$), the external load changes, $\Delta\lambda \neq 0$, and $\Delta t = 0$. On the contrary, during the sustained loading phase, the behaviour of the process zone is assumed to be time-dependent ($\boldsymbol{Q} \neq \boldsymbol{0}$), the external load is kept constant, $\Delta\lambda = 0$, and $\Delta t \neq 0$.

6 INTERACTION BETWEEN COHESIVE ELEMENTS

During the loading phase all the stress path in the FPZ are forced to follow the stress vs. COD law (see Fig. 4 and Eq. 11). For the boundary condition analysed in the present paper, no interaction problem occurs during the loading phase and the condition $dw > 0$ is *always and everywhere* satisfied.

A different situation occurs during the next loading phase (*sustained*). The unloading stiffness, computed as shown in Fig. 5 tends to ∞ when w tends to 0^+.

In order to prevent numerical problems, a threshold value need to be assumed for w. A cohesive element is classified as *active*, and submitted to the rheological model, when and only when its w is bigger than the threshold, assumed equal to $0.018 w_c$. Otherwise the stress path is forced to follow the stress vs. COD law as it occurs during the loading phase.

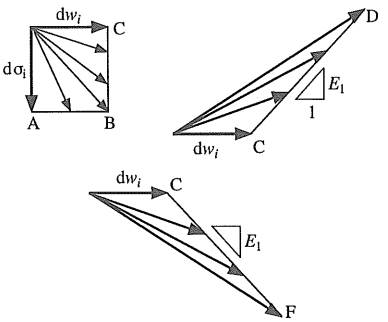

Figure 6: Possible stress and displacement increments.

According to the rheological model, for each active cohesive element, it is possible to compute the stress relaxation under constant w ($\mathrm{d}\sigma_i$) as well as the creep displacement under constant σ ($\mathrm{d}w_i$). Goal of the interaction analysis is to compute the real value of $\mathrm{d}\sigma$ and dw wich must be compatible with global Eq. 12 and with the local $\mathrm{d}\sigma_i$ and $\mathrm{d}w_i$.

The compatibility conditions can be grouped in the following cases :

1. full relaxation only: $\mathrm{d}\sigma = \mathrm{d}\sigma_i < 0$ and $\mathrm{d}w < \mathrm{d}w_i$ (see segment AB in Fig. 6);
2. full creep only: $\mathrm{d}\sigma < \mathrm{d}\sigma_i < 0$ and $\mathrm{d}w = \mathrm{d}w_i$ (see segment BC in Fig. 6);
3. full creep with elastic increment: $\mathrm{d}\sigma = (\mathrm{d}w - \mathrm{d}w_i)E_1 > 0$ and $E_1 > 0$ and $\mathrm{d}w > \mathrm{d}w_i$ (see segment CD in Fig. 6);
4. full creep with softening increment: $\mathrm{d}\sigma = (\mathrm{d}w - \mathrm{d}w_i)E_1 < 0$ and $E_1 < 0$ and $\mathrm{d}w > \mathrm{d}w_i$ (see segment CF in Fig. 6).

In order to follow this process of classification, an inner loop must be introduced. Since the incremental problem is formulated as linear with threshold, each *physical* time step has to be divided in numerous *logical* substeps. When case (3) or (4) are applied, the

matrix coefficients of Eq. 12 are changed from one substep to the next. Otherwise it is kept constant during all the substep iterations. For such a problem it is not possible to prove, in general, the existence and uniqueness of the solution.

During the numerical simulation of three-point bending tests, the following conditions have been satisfied:

1. each cohesive stress relaxation ($d\sigma \leq 0$) induces everywhere $dw > 0$,
2. dw is an increasing function of the distance, computed along the FPZ, starting from the fictitious crack tip;
3. all cohesive elements at the beginning are classified in group (1), i.e., full relaxation only. Afterwards group (2) starts to appear and so on for groups (3) and (4);
4. the fictitious process zone can be divided in two parts. In the first part, located near the fictitious crack tip, all elements are fully relaxed (condition (1) above). In the second part, located near the real crack tip, one of the remaining three conditions is applied.

Since these preliminary conditions are veryfied, the following strategy leads to a solution:

1. the element near the fictitious crack tip is full relaxed, the condition $dw < dw_i$ is verified everywhere;
2. the above operation is repeated moving towards the real crack tip;
3. as soon as the real crack tip reaches the condition of "full creep with elastic increment", its positive stiffness is added and the relaxation procedure is carried on. At this time the boundary between the two above mentioned parts of the FPZ starts to exist;
4. as soon as the previous condition is reached by the element near the real crack tip, the same procedure is applied and the above mentioned boundary moves toward the fictitious crack tip;
5. each time a cohesive element enters in the "full creep with softening increment" condition, the smallest eigenvalue of matrix $(\boldsymbol{K}_T + \boldsymbol{C}_T)$ decreases. Creep rupture time is reached when it becomes negative . From that time on, the external load can no longer be kept constant.

7 THREE-POINT BENDING TESTS

The experimental tests, executed on prenotched beams, described by Zhou (1992), were simulated numerically.

The experimental procedure is based on two phases:

- the external load grows from zero to the nominal level (a fraction of the maximum load P_{max}) under deflection control (5×10^{-6} m/s);
- the load is kept constant until the creep rupture occurs.

These tests are usually associated with the name of *pre-peak sustained bending* tests. Of course, in order to know the maximum load $P_{max} \approx 900$ N, a number of static tests have to be previously executed. To overcome this problem, different authors preferred to use the so-called *post-peak* tests where the creep phase starts beyond the peak point (see Carpinteri et al. (1997) and Barpi et al. (1999)).

The specimen dimensions are $10 \times 10 \times 80$ cm, the notch depth is 5 cm, while the material properties, as decribed in Zhou (1992), are presented in Table 1:

Table 1: Material properties.

E (GPa)	ν (-)	$\mathcal{G}_F$ (N/m)	f_t (MPa)
36	0.10	82	2.8

8 COMPARISON BETWEEN EXPERIMENTAL AND NUMERICAL RESULTS

The numerical simulations were executed using the values listed in Table 1 and Table 2, and neglecting the time dependent behaviour of the undamaged material. The finite element mesh published by Barpi and Valente (1998) were used. Since the above mentioned behaviour starts when the stress reaches a significant level, time zero of each cohesive element precedes the arrival time of the fictitious crack tip. It has been set $\frac{\tau_1}{100}$s before the beginning of the sustained loading phase.

Table 2: Numerical parameters (constant strain elements).

w_c (mm)	τ_1 (s)	$\Delta t/\tau_1$ (-)	β (-)	Element size (mm)
$2.2\ 10^{-4}$	150	1/50	0.05	2.50

Figure 7 shows the load level vs. the logarithm of the failure lifetime (creep rupture time), for different values of the fractional derivative order α. The best fitting of the experimental results is achieved assuming $\alpha = 0.3$. Experimental and numerical results appear to be in good agreement.

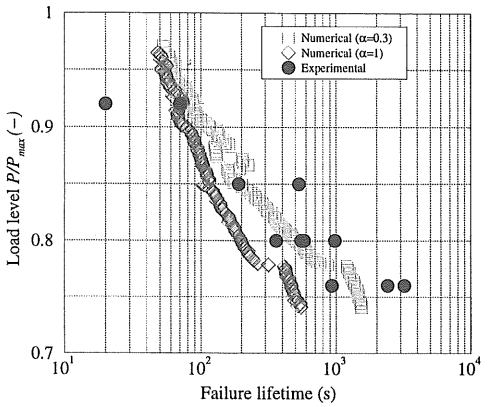

Figure 7: Experimental and numerical load level vs. failure lifetime.

CONCLUSIONS

- A realistic non-linear behaviour at global level *does not require* necessarily a *non-linear model* at local level. A linear viscoelastic rheological element, combined with a suitable micromechanical model can be used.

- To achieve the above mentioned goal, a new time integration scheme is proposed. The incremental problem is formulated as linear with threshold.

- A fractional order rate law has been shown to be a useful tool that makes possible to include a *whole spectrum* of dissipative mechanisms in a single viscous element.

- It is also useful to include an upper limit to the initial values of the unloading stiffness (when $\sigma \approx f_t$). When the hypothesis of linear unloading towards the origin predicts a larger value, the time dependent behaviour is neglected and the stress path is kept on the static curve (σ vs. COD).

- When the time dependent behaviour of the undamaged material is neglected, in order to make up for this simplification, in each point of the fictitious process zone, the zero value of time has been assumed before the arrival time of the fictitious crack tip.

ACKNOWLEDGMENTS

The financial support provided by the Department of University and Scientific and Technological Research (research project on *"Structural Integrity Assessment of Large Dams"*, grant number 9808160821_004) is gratefully acknowledged.

REFERENCES

Bagley, R. L. and P. J. Torvik (1983). Fractional calculus - a different approach to the analysis of viscoelastically damped structures. *AIAA Journal 21*, 741–748.

Barenblatt, G. I. (1959). The formation of equilibrium cracks during brittle fracture: general ideas and hypotheses. *Journal of Applied Mathematics and Mechanics*, 622–636.

Barpi, F., F. Chillè, L. Imperato, and S. Valente (1999). Creep induced cohesive crack propagation in mixed mode. In D. Durban and J. R. A. Pearson (Eds.), *Non-Linear Singularities in Deformation and Flow*, The Netherlands, pp. 155–168. Kluwer Academic Publishers.

Barpi, F., G. Ferrara, L. Imperato, and S. Valente (1999). Lifetime of concrete dam models under constant loads. *Materials and Structures 32*, 103–111.

Barpi, F. and S. Valente (1998). Crack propagation under constant load: constitutive laws for the process zone. In R. de Borst, N. Bićanić, H. Mang, and G. Meschke (Eds.), *Computational Modelling for Concrete Structures*, Rotterdam (The Netherlands), pp. 285–290. Balkema.

Barpi, F., S. Valente, G. Ferrara, and L. Imperato (1998). Experimental and numerical evaluation of gravity dam models failure lifetime. In H. Mihashi and K. Rokugo (Eds.), *Fracture Mechanics of Concrete and Concrete Structures*, Germany, pp. 1615–1624. Aedificatio Publishers.

Bažant, Z. P. and R. Gettu (1992). Rate effects and load relaxation in static fracture of concrete. *American Concrete Institute Journal 89*(5), 456–468.

Bažant, Z. P. and M. Jiràsek (1993). R-curve modeling of rate and size-effects in quasibrittle fracture. *International Journal of Fracture 62*, 355–373.

Bocca, P., A. Carpinteri, and S. Valente (1991). Mixed-mode fracture of concrete. *International Journal of Solids and Structures 27*, 1139–1153.

Carpinteri, A. and F. Mainardi (1997). *Fractals and Fractional Calculus in Continuum Mechanics*. Wien: Springer.

Carpinteri, A., S. Valente, F. P. Zhou, G. Ferrara, and G. Melchiorri (1995). Crack propagation in concrete specimens subjected to sustained loads. In F. H. Wittmann (Ed.), *Fracture Me-*

chanics of Concrete Structures, Germany, pp. 1315–1328. Aedificatio.

Carpinteri, A., S. Valente, F. P. Zhou, G. Ferrara, and G. Melchiorri (1997). Tensile and flexural creep rupture tests on partially-damaged concrete specimens. *Materials and Structures 30*, 269–276.

Dugdale, D. S. (1960). Yielding of steel sheets containing slits. *Journal of Mechanics and Physics of Solids 8*, 100–114.

Enelund, M., L. Mähler, K. Runesson, and B. Lennart Josefson (1999). Formulation and integration of the standard linear viscoelastic solid with fractional order rate laws. *International Journal of Solids and Structures 36*, 2417–2442.

Gel'fand, I. M. and G. E. Shilov (1964). *Generalized Functions, Volume I, Properties and Operations*. San Diego: Academicy Press.

Hansen, E. A. (1991). Influence of sustained load on the fracture zone of concrete. In J. G. M. van Mier, J. G. Rots, and A. Bakker (Eds.), *Fracture Processe in Concrete Rock and Ceramics*, pp. 829–838. E&FN Spon.

Hillerborg, A., M. Modeer, and P. E. Petersson (1976). Analysis of crack formation and crack growth in concrete by means of fracture mechanics and finite elements. *Cement and Concrete Research 6*, 773–782.

Huang, J. and V. Li (1989). A meso-mechanical model of the tensile behaviour of concrete. *Composites 20*, 370–378.

Karihaloo, B. L. (1995). *Fracture Mechanics and Structural Concrete*. England: Longman Scientific and Technical.

Oldham, K. B. and J. Spanier (1974). *The Fractional Calculus*. New York: Academicy Press.

Santhikumar, S. and B. L. Karihaloo (1996). Time-dependent tension softening. *Mechanics of Cohesive-Frictional Materials 1*, 295–304.

Santhikumar, S., B. L. Karihaloo, and G. Reid (1998). A model for ageing visco-elastic tension softening material. *Mechanics of Cohesive-Frictional Materials 3*, 27–39.

Wu, Z. S. and Z. P. Bažant (1993). Finite element modeling of rate effects in concrete with influence of creep. In Z. P. Bažant and I. Carol (Eds.), *Creep and Shrinkage of Concrete*, London, pp. 427–432. E&FN Spon.

Zhou, F. P. (1992). *Time-dependent crack growth and fracture in concrete*. Ph. D. thesis, Report TVBM-1011, Lund University.

Zhou, F. P. and A. Hillerborg (1992). Time-dependent fracture of concrete: testing and modelling. In Z. P. Bažant (Ed.), *Fracture Mechanics of Concrete Structures*, The Netherlands, pp. 906–911. Elsevier Applied Science.